Phase Behavior of a Lipid/Polymer−Lipid Mixture in Aqueous Medium

ARTICLE *in* MACROMOLECULES · JULY 1995

Impact Factor: 5.8 · DOI: 10.1021/ma00108a029

2 AUTHORS, INCLUDING:

David Needham
Duke University
12 PUBLICATIONS **1,089** CITATIONS

SEE PROFILE

Phase Behavior of a Lipid/Polymer−Lipid Mixture in Aqueous Medium

Kalina Hristova*,† and David Needham

Department of Mechanical Engineering and Materials Science, Duke University, Durham, North Carolina 27708

Received February 22, 1994; Revised Manuscript Received November 14, 1994⊗

ABSTRACT: The phase behavior of a mixture of bilayer forming lipids and polymer−lipids (lipids with covalently attached polymer to their hydrophilic moieties) in excess water is studied theoretically. The mixture is predicted to exhibit complex phase behavior for polymer molecular weights 2000 and 5000, depending on the concentration (fraction) of polymer−lipids in the lipid mixture. The bilayer is characterized by a maximal concentration n_{sat} (saturation limit) of polymer−lipids that it can incorporate, as determined by its material properties (elastic modulus of area expansion and critical area expansion). At a different concentration n_{tr}, which we call the thermodynamics crossover, micelle formation becomes energetically favorable over bilayer formation. We show that for DSPC and SOPC bilayers $n_{tr} < n_{sat}$. Increase of the polymer−lipid concentration above n_{tr} leads to a gradual transition from a bilayer to a micellar phase; bilayers and micelles can coexist. In the transition region the polymer−lipid concentration is higher in the micellar phase than in the coexisting bilayer.

1. Introduction

The behavior of solvated adsorbed or grafted polymers at the interface between biofluids and biomaterials is currently attracting attention because of the unique repulsive properties that these polymers possess. For example, a strategy based on a polymer-grafted lipid that can be incorporated into lipid bilayers is leading to a more effective intravenous liposome drug delivery system.[1−11] The presence of polymer (poly(ethelene glycol) or PEG) at the bilayer surface in these systems gives rise to steric interactions that appear to stabilize the lipid bilayer against the close approach of other macromolecules and cells, thus increasing blood circulation time and allowing targeting to solid tumors.

These polymer-grafted vesicles are formed spontaneously as a result of the rehydration of the polymer−lipid/lipid mixture when the concentrations of polymer−lipid in the lipid mixture are low (less than 15 molar % (M %)).[12,13] At the other extreme, a 100% polymer−lipid in water forms micelles.[12] This implies that the lipid/PEG−lipid/water system has a complex phase behavior. It needs to be studied for the sake of biomaterials design. The conditions under which bilayers (i.e. vesicles) are formed have to be determined.

The polymer-grafted bilayer system can be considered as consisting of two components: a lipid bilayer and polymer layer(s)[14,15] (see Figure 1). The structure and basic physical properties of each of the two components as separate entities have been studied. For instance the properties of polymers, grafted to solid surfaces,[16−20] copolymer bilayers,[21] diblock copolymer monolayers,[22] and block copolymer microemulsions[23] have been discussed.

Also there are a lot of papers which refer to the bending modulus of the lipid bilayer and thus to its structure and molecular organization.[24−28] These studies have been extended to lipid monolayers[29−32] and lipid micelles.[33−37]

A number of phase transitions from one molecular self-organized structure to another have been predicted for block copolymer melts[38−40] and solutions.[41,42] Dan and Safran[43] show that a mixture of two diblock copolymers can lead to destabilization of the lamellar bilayer.

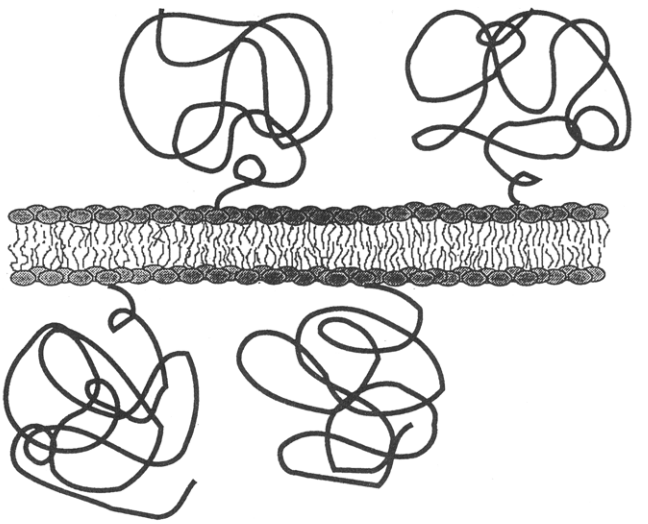

Figure 1. Schematic diagram showing a polymer-grafted bilayer at low grafting concentrations, where the polymer assumes a "mushroom" conformation.

The studies of phase transitions between different aggregates of lipid molecules are based mainly on some phenomenological models.[44,45] These models give a good idea how the structure of the molecules determines the size and shape of the aggregate and how mixing of two types of molecules can promote the formation of a new type of aggregate. For instance Safran *et al.*[46] discuss how a mixture of two surfactants, which individually form micelles or bilayers can form vesicles of a particular kind.

The analysis of Safran *et al.*[46] has some relevance to the system we are studying because this system is a mixture of bilayer-forming lipids and PEG−lipids, which form micelles on their own. Yet to treat the system as a pure lipid system will be a crude simplification, since the grafted polymer has its own specificities. As already mentioned, the polymer-grafted lipid system has a lipid and a polymer component. We assume that the two

† Present address: Department of Physiology and Biophysics, University of California−Irvine, Irvine, CA 92717-4560.

⊗ Abstract published in *Advance ACS Abstracts,* January 15, 1995.

0024-9297/95/2228-0991$09.00/0

components are relatively independent, i.e. the basic physics of the two components is not much changed. Yet they influence each other and it is this mutual influence that drives the phase transitions that we will consider.

The suggested approach merges membrane biophysics and polymer physics into a coherent study to address the basic physical properties of the man-made polymer-lipid system. This is the approach we have used previously to study the mechanical and interactive properties of polymer-grafted bilayers.[14,15]

In this paper, using a relatively easy analysis and without very difficult calculation we show that the PEG–lipid can destabilize the lipid bilayer. The paper sends a message to the liposome companies since using the formalism, presented here, one can optimize the composition of the drug-carrying liposomes.

As we will show, the complexities in the phase diagram of the polymer–lipid/lipid/water system in excess water is determined by the self-assembling properties of the lipids. Two factors influence the nature of the phase behavior.

(1) *Material properties of the bilayer.* The presence of grafted polymer induces bilayer deformations which cannot exceed certain critical values without causing the rupture of the bilayer.

(2) *Lipid polymorphism.* Lipid molecules can form different types of aggregates under different conditions (for instance water content, temperature, and as we will discuss here, concentration of incorporated polymer–lipid[47]. Here we are considering phospholipids, which under normal conditions (room temperature, pH = 7, and excess water) form bilayer structures.

We will study the phase behavior of the polymer–lipid/lipid mixture in excess water as a function of the concentration (fraction) of the polymer–lipid in the lipid mixture. Special attention will be paid to the cases when a bilayer is formed. We will study the phase behavior for poly(ethelene glycol) molecular weights 2000 and 5000, products which are used in the preparation of drug-carrying liposomes for therapeutical purposes.[4,7–11]

We will show that the critical material properties such as the elastic modulus of area expansion and maximum area expansion of the bilayer determine a maximum polymer–lipid concentration in the bilayer. Lipid polymorphism is a factor in the distribution of the material between the two phases—bilayer and micellar; i.e. the two phases can coexist or one can prevail. Increasing the polymer–lipid concentration can have two effects: (1) the micellar phase can become more energetically favorable than the bilayer phase or (2) the bilayer concentration can reach its absolute maximum, which is defined by the critical material properties of the bilayer. The structure of the bilayer and the polymer molecular weight determine which effect occurs first.

1.1. The Lipid Bilayer as a Self-Organized Structure. Amphiphilic molecules (built up of two distinct parts—a polar region and an apolar region) in aqueous media spontaneously self-assemble into aggregates. This occurs when the concentration exceeds a critical one (CMC) (for instance, for DSPC CMC is on the order of 10^{-12} M).[48] These aggregates can have different shapes (spherical, cylindrical, flat) and sizes, depending on the structure of the molecules and their concentration. The common feature of the aggregates is that the polar (or hydrophilic) parts of the molecules are exposed to water and the apolar (or hydrophobic) parts are packed together and hidden inside the aggregate. The driving force for this self-assembly is an entropy-driven effect, called the hydrophobic effect.[49] It stems from the fact that immersing a hydrophobic object into a highly polar medium (such as water) leads to the arrangement of the water molecules around the object and thus to a decrease in the entropy of the system.

As discussed by Israelachvili,[44] fully hydrated lipid molecules such as DSPC, EggPC, etc., which have a predominantly cylindrical shape (the area per head equals the area per tail), will form bilayers.

A bilayer exists mainly due to the fact that it is excluded from the solvent, since its molecules are not strongly bound. This is quantitatively manifested in its low elastic coefficients, the bending rigidity k_c (of the order of several kT), and the area expansion modulus K_A, which will be discussed here in detail.

The response of the bilayer surface area A to an isotropic tension $\bar{T}$ is specified by the isothermal modulus of surface compressibility:

$$K_A = A\left(\frac{\partial \bar{T}}{\partial A}\right)_T \tag{1}$$

Typical values for the area compressibility modulus of fluid bilayers are $K_A \sim 0.2$ N m^{-1} or 200 dyn/cm.[50] If we convert it into an equivalent bulk modulus by dividing by the membrane thickness ~5 nm, we get a compressibility $\sim 10^7$ N m^{-2}, which is somewhere between that of an ordinary liquid and a gas. So we can view the membrane as a two-dimensional liquid that can be about 1000 times more compressible than its embedding fluid. Bilayer compressibility varies with lipid phase (gel versus liquid) and lipid composition, especially cholesterol content.

Increasing the cholesterol content (up to 50%) increases bilayer cohesion and changes bilayer physical properties (for instance it can increase K_A by 1 order of magnitude). Thus varying the amount of cholesterol in the bilayer provides us with a simple means to vary the mechanical parameters (elastic constants, etc.) of bilayers.

At a certain applied lateral tension τ_s a sudden and unavoidable membrane rupture occurs. At the point of rupture the membrane is characterized by its maximal area change. Expansions, larger than this cannot be achieved. The elastic modulus of area expansion of the bilayer and the maximum area change have been measured in micropipet experiments for liquid bilayers[51a] as a function of cholesterol content and for gel-phase bilayers.[52] [The elastic modulus of area expansion of the bilayer and its maximum area change $\Delta A/A$ will be referred to here as critical material parameters of the bilayer.] The mechanism of rupture of pure gel-phase bilayers depends on the nature of the defects and is not as well understood.

Bilayers can undergo also substantial changes with temperature. Above a certain transition temperature the bilayer exists as a two-dimensional liquid. Below this temperature the bilayer is a two-dimensional solid. The molecules are tightly packed in a crystal lattice. As compared to liquid bilayers K_A for gel-phase bilayers increases more than 5 times.[52] Nevertheless, the crystal lattice is more brittle and fragile than an ordinary solid material and can support lots of defects because it is held together by weak van der Waals forces. The transition temperature varies with the chemical composition and hydration level of the membrane.

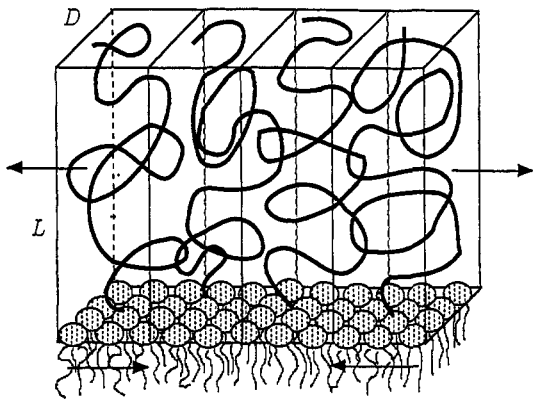

Figure 2. Schematic diagram showing a polymer brush. Polymer lateral pressure is balanced by bilayer cohesion.

The hydration of a mixture of polymer–lipids and lipids will also lead to their spontaneous assembly into aggregates. If the hydrocarbon tails of the lipids and polymer–lipids are identical, one could expect the two types of lipids to mix well. In the aggregates the hydrocarbon tails will be packed together and the heads with the long hydrophilic polymer chains will be exposed to water. Since PEG does not adsorb on lipid surfaces[53] it will remain attached to the bilayer in only one point (grafted to the bilayer). The chain will extend into the aqueous medium, thus maximizing its interaction with the solvent.

If polymer is grafted on a **solid** surface the lateral repulsion between the polymer chains is unlikely to have any effect on its structure since solids are held together by strong chemical forces. On the contrary, in the lipid bilayer lateral polymer chain repulsion may create curvatures, area expansion, or even mechanical breakdown due to the low elastic coefficients and weak bonds between the molecules. To understand the influence of the polymer on the bilayer we have to characterize the polymer system itself.

The behavior of grafted polymer chains was first studied by Alexander[16] and de Gennes.[17] According to them, two concentration regimes can be identified for the polymer chains at the surface, and the physical characteristics of the polymer system are different in these two regimes. When the grafting density is low, the chains form separate "mushrooms", each with a size $R_F \cong aN^{3/5}$, where N is the degree of polymerization and a is the monomer size. [In polymer theories the term "monomer" is used for the repeat unit in the polymerized chain. It is referred to as "mer" in materials science.] Such a situation is shown for a polymer–lipid bilayer system in Figure 1. When the grafting level is high, the chains overlap laterally to form a continuous "brush" and the polymer system can now be considered a semidilute solution. The brush regime is shown for one monolayer of a bilayer in Figure 2. The most advanced "brush" theory is the mean field theory of Milner, Witten, and Cates.[18–20,54] which we will discuss here in brief.

1.2. Self-Consistent Theory for Polymer Brushes. This theory refers to grafted chains of high molecular weight, strongly stretched relative to their unperturbed radius.[18–20,54]

Miner, Witten, and Cates show that the chain configuration can be described as a trajectory of a fictitious particle, moving toward the plane of the surface in a potential U. $U = -vc$, where c is the monomer concentration and v is the so-called excluded volume, which characterizes the monomer–monomer interactions in a solvent.[55] U is the mean-field potential in which the chain is embedded. It is due to the presence of the other chains grafted on the surface. Then Milner, Witten, and Cates show that the time integral along the path of the particle is equal to N and argue that all particles must reach the wall in the same time, regardless of their starting point. If the free ends of the chains are distributed with non-zero density over the entire height of the brush, the effective potential has to be that of a harmonic oscillator: $-U(z) = A - Bz^2$. (The period of a particle moving in such potential is independent of the amplitude of motion.) Since $U = -vc(z)$ it can be easily seen that the density profile is a parabolic one, as opposed to the step function of de Gennes.[17]

The period of a harmonic oscillator with unit mass and "spring constant" $2B$ is $\tau = 2\pi(2B)^{-1/2}$. The path of the fictitious particle is a one-quarter cycle, so $\tau = 4N$ and

$$B = \frac{\pi^2}{8N^2} \tag{2}$$

The constant A is found by computing the net amount of material in the brush

$$N\sigma = \int_0^L \mathrm{d}z\, c(z) \tag{3}$$

which gives

$$A(L) = \frac{N\sigma v}{L} + \frac{BL^2}{3} \tag{4}$$

[Here the parameters are dimensionless: the lengths are scaled by the monomer size a and the energies are scaled by kT.]

From the requirement that $c(z) = -U/v$ is non-negative the maximal extension from the surface can be found:

$$L_{max} = (A(L_{max})/B)^{1/2} \tag{5}$$

Now the energy of this parabolic brush can be computed. First, Milner *et al.*[20] note that the chain energy is stationary with respect to the end position. The brush can be constructed by progressively adding chains. So they consider a chain which starts very close to the surface and has no stretch energy. The free energy to add such a chain is AN and the average free energy per chain for known surface coverage σ is given by

$$F_{MWC} = \frac{1}{\sigma}\int_0^\sigma \mathrm{d}\sigma'\, S(\sigma') = \frac{9}{10}(\sigma v)^{2/3}(\pi^2/12)^{1/3}N \tag{6}$$

In the case of athermal solvent, $v = a^3$. Instead of the dimensionless surface coverage σ, in this paper the density of grafting will be quantitatively described by the distance between points of grafting D: $\sigma = a^2/D^2$. Then eq 6 can be written in units of energy as

$$F_{MWC} = \frac{9}{10}kT\left(\frac{\pi^2}{12}\right)^{1/3}N\frac{a^{4/3}}{D^{4/3}} \tag{7}$$

where N is the degree of polymerization, a is the monomer size, and D is the distance between points of grafting.

2. Saturation Limit of the Polymer in the Bilayer Determined by Its Critical Material Parameters

After these introductory arguments we can now calculate the maximal concentration of polymer–lipid that can be incorporated in a bilayer.

We define the saturation limit of the polymer–lipid in the bilayer n_{sat} as the maximal fraction of polymer–lipids that can be incorporated in the bilayer. To derive this saturation limit we note that since by definition there are no lateral interactions between polymers in the mushroom regime the saturation limit should not occur until polymer concentrations are within the brush regime. [Although this is correct only for gel-phase bilayers, as we will show later, the lateral pressures in the mushroom regime for liquid crystalline bilayers are small and the saturation limit will also occur in the brush regime.]

The area dilation due to the grafted polymer brush will be opposed by the cohesive forces between the lipid molecules (see Figure 2). As a result, the degree of expansion will depend on the elastic constant of area expansion K_A, which is a quantitative characteristic of the bilayer cohesion. We expect then that we can control and manipulate this maximum concentration by changing the lipid composition (e.g. incorporating cholesterol that is known to increase the toughness of the bilayer[51] and the polymer molecular weight.

To calculate n_{sat} we assume that the free energy of the polymer-grafted bilayer is the sum of the energy stored in the polymer brush and the elastic energy of the bilayer. Then the equilibrium area dilation is the one which minimizes the energy sum. The critical polymer concentration (at saturation) is the one for which the equilibrium area dilation equals the maximum one since larger concentrations are impossible to achieve.

Let us consider a square patch of the bilayer with side D, where D is the distance between grafting points in the bilayer. Due to the area expansion as a result of polymer lateral pressure

$$D^2 = D_1^2 + \Delta D^2 \tag{8}$$

where D_1 is the distance between grafting points in a pure lipid bilayer (or in a bilayer with $K_A = \infty$). The parameter ΔD^2 is given by

$$\frac{\Delta D^2}{D_1^2} = \frac{\Delta A}{A} \tag{9}$$

where ΔA is the area change due to polymer lateral tension and A is the area per lipid molecule in a pure unstretched lipid bilayer.

The patch will represent the bilayer area covered by one polymer chain. The elastic energy of this patch to the second order of ΔA is[50]

$$F_{el} = \frac{K_A}{2}\frac{(\Delta A)^2}{A^2} D_1^2 \tag{10}$$

The energy of the two polymer chains of the brush (one polymer per monolayer) will be[18,19]

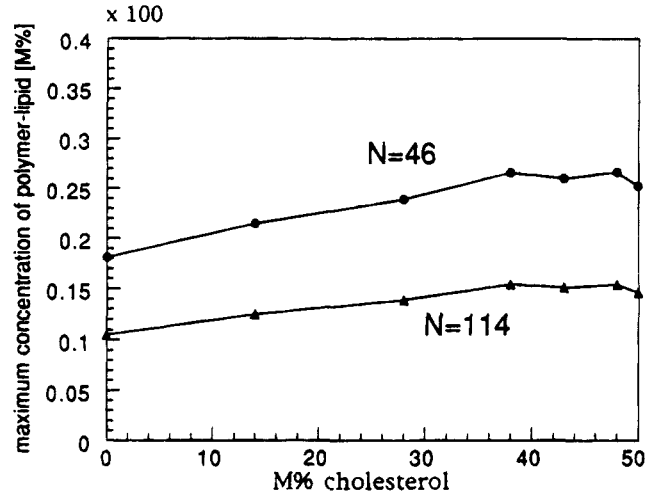

Figure 3. Maximum concentration of polymer–lipid that can be incorporated in the bilayer n_{sat} as a function of cholesterol content in the bilayer.

$$F_{MWC} = 2\frac{9}{10}kT\left(\frac{\pi^2}{12}\right)^{1/3} N\frac{a^{4/3}}{D^{4/3}} =$$

$$\frac{9}{5}kT\left(\frac{\pi^2}{12}\right)^{1/3} N\left(\frac{a^{2/3}}{D_1^{2/3}}\right)^2 \left(1 - \frac{2}{3}\frac{\Delta A}{A} + \frac{5}{9}\frac{(\Delta A)^2}{A^2}\right) \tag{11}$$

The free energy of the bilayer patch $F_{bil} = F_{el} + F_{MWC}$ is minimized for

$$\frac{\Delta A}{A} = \frac{\frac{6}{5}kT\left(\frac{\pi^2}{12}\right)^{1/3} N\left(\frac{a^2}{D_1^2}\right)^{2/3}}{K_A D_1^2 + 2kT\left(\frac{\pi^2}{12}\right)^{1/3} N\left(\frac{a^2}{D_1^2}\right)^{2/3}} \tag{12}$$

where D_1 is related to the saturation concentration n_{sat} (fraction of polymer–lipids in the lipid mixture) as

$$\frac{n_{sat}}{A} = \frac{1}{D_1^2} \tag{13}$$

The solution of (12) for D_1 gives n_{sat} as a function of K_A and $\Delta A/A$, two characteristic material parameters of the bilayer.

$$n_{sat} = \frac{A}{a^2}\left(\frac{\Delta A}{A}\frac{K_A a^2}{kT}\frac{1}{\left(\left(\frac{\pi^2}{12}\right)^{1/3} N\left(\frac{6}{5} - 2\frac{\Delta A}{A}\right)\right)}\right)^{3/5} \tag{14}$$

We use $a = 3.5$ Å[51b] and values of K_A and $\Delta A/A$ from micropipet measurements[51a] to predict the maximum concentration of polymer–lipid in the bilayer. The prediction is plotted in Figure 3 as a function of cholesterol content in the SOPC bilayer.

The saturation concentration due to the material properties gives the absolute limit of polymer concentration in the bilayer. But as we will show below, the bilayer phase may cease to exist at concentrations lower than just predicted due to a phase transition from the lamellar to the micellar phase.

Before discussing the phase transitions themselves we first must construct the free energy of different phases of the polymer–lipid/lipid solutions. The phase with the lowest energy should represent the equilibrium

phase, and the free energy difference between the phases should give information about the possible coexistence of different phases.

If A and B are two phases with energies E_A and E_B, then the probabilities P for their occurrence will be connected through

$$\frac{P(A)}{P(B)} = \exp(E_B - E_A)/kT \qquad (15)$$

If $E_A - E_B$ is of the order of kT, they can coexist; if $E_A - E_B \ll 1$ or $E_A - E_B \gg 1$, then only one phase will exist.

3. Free Energy of Possible Polymer–Lipid/Lipid/Water Phases

3.1. Gel-Phase Bilayers. As already discussed, in the gel phase the chains are tightly packed in an all-trans conformation. The bilayer is a two-dimensional solid. A typical lateral diffusion coefficient for the gel-phase is 10^{-10} cm^2/s, compared to 10^{-8} cm^2/s[48] for liquid bilayers. In our theoretical treatment we will consider two systems—one with no lateral mobility at all and another in which the molecules freely diffuse in the lateral direction. This will enable us to see the effect of fluidity of the bilayer. Also, we relate our findings for the immobile bilayer to gel-phase bilayers and the one with free diffusion to the liquid system. We will use the parameters for DSPC and SOPC bilayers for the gel-phase and liquid crystalline case, respectively.

If we assume that diffusion does not occur in the system, then the polymer will be attached to one point of the surface. Next we assume that the polymer–lipids are homogeneously distributed throughout the bilayer. The distance between the grafting points is fixed, equal to D ($D^2 = A/M$, where A is the area of the lipid molecule in the bilayer and M is the molar fraction of the polymer–lipids).

If there is no lateral diffusion and the mushrooms are homogeneously distributed throughout the bilayer, there will be no lateral interactions between the mushrooms. So the regime in which phase transitions are expected to occur is the brush regime. Let us consider the energy of a patch of membrane, covered by one polymer for fixed molar percent polymer–lipid (M = constant) under the assumption that the system is in the brush regime (Figure 4). In the brush regime there is energy, stored in the brush which increases with the molecular weight of the polymer and the grafting concentration. This stored free energy is expressed in the lateral tension between the brushes. There are two possible mechanisms by which this pressure could be relaxed.

One mechanism involves curving the grafting surface. The higher the curvature, the bigger the pressure relaxation. The highest curvature will be obtained if the lipids pack into micelles (cylindrical or spherical) (Figure 5). Since the lipids we are considering form bilayers under normal conditions, there will be additional energy cost due to "unfavorable packing" of the hydrocarbon chains in the micelles. While the latter energy does not depend on the molecular weight and grafting density, the energy stored in the polymer brush will depend crucially on them. One can expect under certain conditions the micelle packing to become more favorable.

A second possible mechanism is to induce some structural changes in the bilayer. Probably the most drastic one is transition to interdigitated bilayer (Figure 6). This phase has been observed for highly charged gel-phase bilayers.[56–58] A prerequisite for the appearance of this phase is strong repulsion between lipid heads, which is present in our system due to the lateral brush steric repulsion. In this phase the area per lipid molecule doubles. This will double the area covered by a polymer brush and relax the lateral pressure. The energy cost associated with the transition to this phase is due to the increased oil–water interface which has an energy density of 50 dyn/cm^2.[59] Below we will

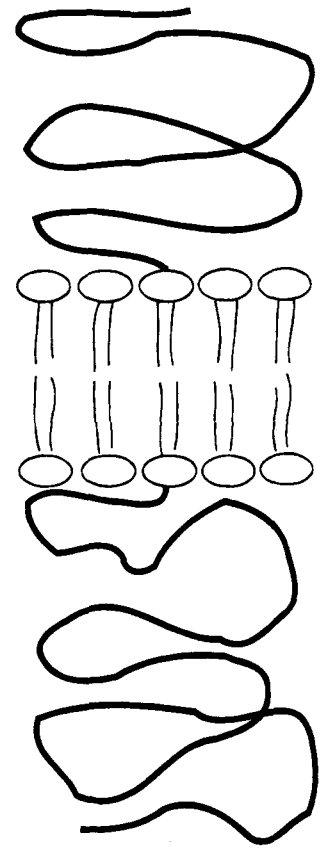

Figure 4. Schematic diagram showing the membrane patch which is considered in the area expansion model (see text).

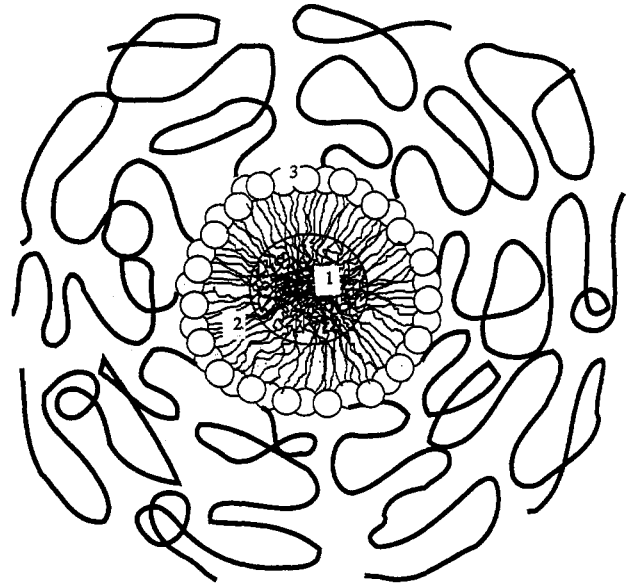

Figure 5. Schematic diagram showing a polymer-grafted micelle: (1) a central core, (2) outer hydrocarbon chains, (3) hydrated headgroups.

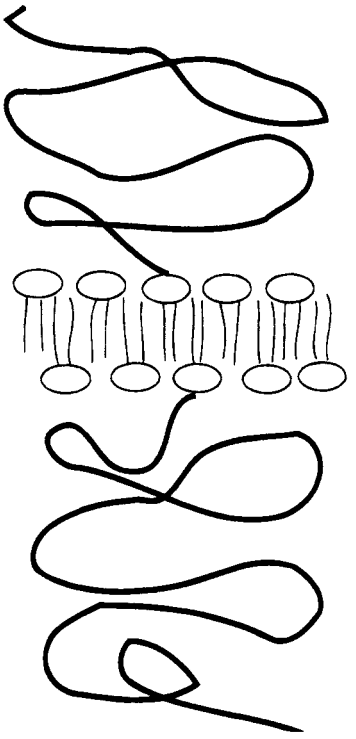

Figure 6. Schematic diagram showing a membrane patch of an interdigitated bilayer.

identify the molecular parameters for which the energy minimum occurs for this interdigitated state.

Now we proceed to construct the free energy of the normal bilayer, the interdigitated bilayer and the micelle. We again consider the polymer with molecular weights 2000 and 5000. The predictions refer only to the brush regime and so they will begin at molar percents M such that $R_F^2 = A/M$. The modeling is valid for any water-soluble polymer. For the numerical predictions we will use the value of $a = 3.5$ Å, which is the monomer size for PEG.

1. Bilayer Phase. The calculation of the free energy of the bilayer is done in analogy to the one in section 2. The free energy of the membrane patch, defined in the previous section (see Figure 4) in its minimum is

$$F_{bil} = \frac{9kT}{5}\left(\frac{\pi^2}{12}\right)^{1/3} N\frac{a^{4/3}}{D_1^{4/3}}\left(1 - \frac{\frac{2}{5}kT\left(\frac{\pi^2}{12}\right)^{1/3} N\left(\frac{a^2}{D_1^2}\right)^{2/3}}{K_A D_1^2 + 2kT\left(\frac{\pi^2}{12}\right)^{1/3} N\left(\frac{a^2}{D_1^2}\right)^{2/3}}\right) \quad (16)$$

Then the free energy of the bilayer phase per one polymer chain F_1 will be half of this value (the considered membrane patch includes two polymer chains):

$$F_1 = \frac{9kT}{10}\left(\frac{\pi^2}{12}\right)^{1/3} N\frac{a^{4/3}}{D_1^{4/3}}\left(1 - \frac{\frac{2}{5}kT\left(\frac{\pi^2}{12}\right)^{1/3} N\left(\frac{a^2}{D_1^2}\right)^{2/3}}{K_A D_1^2 + 2kT\left(\frac{\pi^2}{12}\right)^{1/3} N\left(\frac{a^2}{D_1^2}\right)^{2/3}}\right) \quad (17)$$

We plot this energy as a function of M% polymer–lipid for the two molecular weights (2000 and 5000) in Figures 7a and 8a for $K_A = 1000$ dyn/cm and $A = 50$ Å^2. As expected, the energy increases with the polymer molecular weight and the concentration of the polymer–lipid in the bilayer.

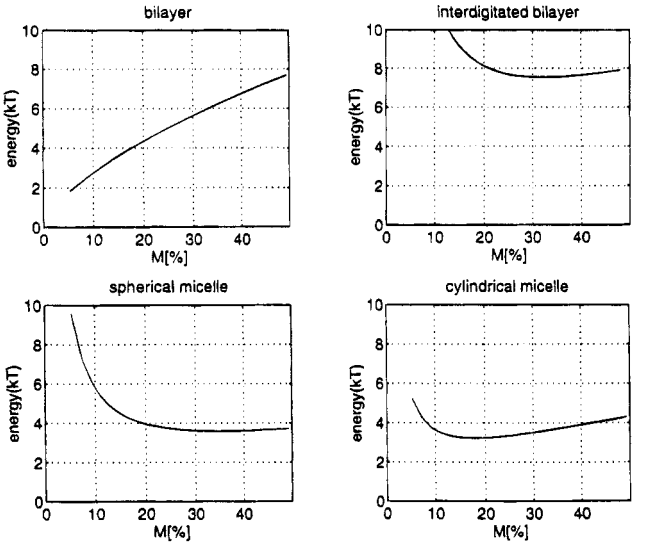

Figure 7. Energy of the lipid–polymer/lipid system per one polymer chain of molecular weight 2000 as a function of M % polymer lipid for gel-phase bilayers ($A = 50$ Å^2, $K_A = 1000$ dyn/cm, $G_{pack}^{sph} = 0.5kT$, $G_{pack}^{cyl} = 0.25kT$, $a = 3.5$ Å): (a) bilayer, (b) interdigitated bilayer, (c) cylindrical micelle, (d) spherical micelle.

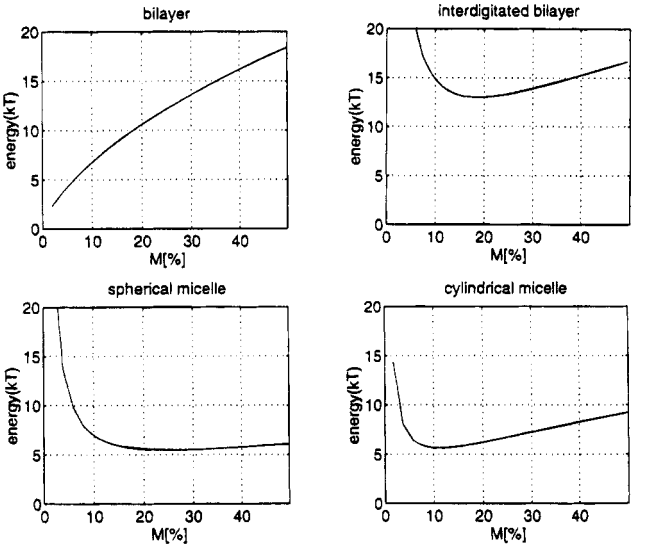

Figure 8. Energy of the lipid–polymer/lipid system per polymer chain of molecular weight 5000 as a function of M % polymer lipid for gel-phase bilayers. ($A = 50$ Å^2, $K_A = 1000$ dyn/cm, $G_{pack}^{sph} = 0.5kT$, $G_{pack}^{cyl} = 0.25kT$, $a = 3.5$ Å): (a) bilayer, (b) interdigitated bilayer, (c) cylindrical micelle, (d) spherical micelle.

Let us note that changes in the concentrations of the polymer–lipids actually change the size of the membrane patch that we are considering. For low concentrations the patch consists of a large number of lipid molecules per one polymer chain. For instance for 5 M % we have one polymer–lipid per 19 lipids, i.e. one chain per 20 lipids. For 20 M % we have one chain per five lipids; the patch is much smaller. It is the relative magnitude of the energy stored in the polymer and the energy stored in the bilayer that are critical to the thermodynamics of the system. The increase of polymer–lipid concentration not only increases the brush energy, but since the membrane portion becomes smaller

the contribution of the bilayer to the free energy decreases.

2. Interdigitated Bilayer Phase. A schematic representation of an interdigitated bilayer is given in Figure 6. In this case we expect $K_A = K'_A/2$ (thinner bilayer), $A' = 2A$, and thus $D' = 2^{1/2}D_1$. So the sum of the stretching F_{str} and polymer energy F_{pol} per one polymer chain can be written as

$$F_{str} + F_{pol} = \frac{9}{10}kT\left(\frac{\pi^2}{12}\right)^{1/3} N\frac{a^{4/3}}{D'^{4/3}}\left(1 - \frac{\frac{2}{5}kT\left(\frac{\pi^2}{12}\right)^{1/3} N\left(\frac{a^2}{D'^2}\right)^{2/3}}{K'_A D'^2 + 2kT\left(\frac{\pi^2}{12}\right)^{1/3} N\left(\frac{a^2}{D'^2}\right)^{2/3}}\right) \quad (18)$$

Next, to obtain the full membrane free energy per one polymer chain F_2 we have to add a term, expressing the energy increase due to increased oil–water interface.

$$F_2 = F_{str} + F_{pol} + F_{oil/w} \quad (19)$$

To evaluate the free energy increase $F_{oil/w}$, we will use a simple method, which was used by Israelachvili[44] to evaluate the optimum molecular area in a fluid bilayer.

The interfacial tension forces act to contract the bilayer, minimizing the interactions of the hydrocarbon tails with water. This energy contribution can be written as γA, where $\gamma = 50$ dyn/cm^2 [59] is the oil–water surface tension. The repulsive contributions come from electrostatic repulsion between charged headgroups, hydration repulsion, steric headgroup and chain interactions. Israelachvili[44] assumes that, as in the two-dimensional van der Waals equation of state, the first term is inversely proportional to the head area A (pressure $\propto 1/A^2$).

Then the interfacial energy is given by

$$G(A) = \gamma A + K/A \quad (20)$$

This energy has minimum for $A_0 = (K/\gamma)^{1/2}$.

In the fluid bilayer $A_0 \propto 65$ Å^2. We can use this value to calculate K from (20). We obtain $K = 2.1125 \times 10^{-27}$ dyn·cm^2. Now let us freeze the system. We can expect that neither of the parameters change substantially. The main difference is that since the chain is frozen the area A can take only values 50 Å^2 (the cross-sectional area of a hydrocarbon chain in the all-trans conformation) for the bilayer and 100 Å^2 for the interdigitated bilayer and thus we obtain: $G(A)$ of 6.725×10^{-13} dyn for the bilayer and $G(2A)$ of 7.1125×10^{-13} dyn for the interdigitated bilayer. Thus the free energy difference between the interdigitated and normal bilayer for one molecule is $\Delta G = 7.1125 \times 10^{-13}$ dyn or $\Delta G = 0.96kT$. Then

$$F_{oil/w} = \Delta G\frac{D^2}{A} = \Delta G/M \quad (21)$$

This energy is to be summed up with the energy stored in the polymer according to (19). We plot F_2, given by (19) as a function of M % polymer–lipid for polymer molecular weights 2000 and 5000 as shown in Figures 7b and 8b for $K_A = 1000$ dyn/cm and $A = 50$ Å^2. The energy F_2 decreases with increasing polymer–lipid concentration. With increasing polymer–lipid concentration, the relative importance of the interfacial energy decreases as the number of lipid molecules per polymer chain decreases. The lateral repulsion between the chains becomes dominant and the interdigitation of the hydrocarbon tails relaxes this repulsion. As a result of this at 50 M % for molecular weight 2000 and 36 M % for molecular weight 5000 the two energies F_1 and F_2 become equal.

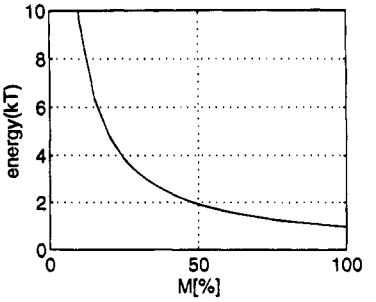

Figure 9. Oil–water interface energy per polymer chain.

This analysis is valid for concentrations of polymer – lipids such that $R_F^2 > 2A/M$; i.e. after the interdigitation the polymer system remains in the brush regime. If $R_F^2 < A/M < 4R_F^2$, the result of the interdigitation will be a transition to the mushroom regime; i.e. the interactions between the chains will go to zero. Then the energy of the system will come only from the pure bilayer. We plot this bilayer energy per polymer chain in Figure 9. In the case $R_F^2 < A/M < 4R_F^2$ it is the comparison between Figure 7a or 8a and Figure 9 that can give us information whether interdigitation is likely to occur. Our results show that interdigitation, leading to a change of polymer regime is not likely to occur for molecular weights 2000 or 5000. For example, for molecular weights 2000 (Figure 7a) at 5 M % ($R_F^2 < A/M < 4R_F^2$ is fulfilled) F_1 is about $3kT$ while F_2 is more than $10kT$. Such interdigitation, however, is likely to occur for low molecular weight polymers, for which R_F is small and so $R_F^2 < A/M < 4R_F^2$ is fulfilled for relatively large molar percents (for example, for poly(ethelene glycol) of molecular weight 350, $R_F^2 < A/M < 4R_F^2$ is fulfilled up to about 30 M %). Then the energy of the interdigitated bilayer F_3 is only several kT and is comparable to the bilayer one F_1.

3. Micellar Phase. First, let us discuss the energy of a polymer brush, grafted on a curved surface.

As discussed by Milner and Witten[60] in terms of their mean-field theory in the bent configuration, the local monomer chemical potential is still parabolic, $-U = A - Bz^2$. The coefficient B must still be given by the "equal time" requirement for the chain conformations, i.e. $B = \pi^2/(8N^2)$. Again

$$c(z) = B(h^2 - z^2) \quad (22)$$

where $c(z)$ is the monomer concentration profile and h is the polymer extension from the surface.

The "mass conservation" law can be written as

$$4\pi \int_R^{R+h} c(z)z^2\, dz = 4\pi R^2 N\sigma \quad (23)$$

where

$$c(z) = B((R+h)^2 - z^2) = \pi^2/(8N^2)((R+h)^2 - z^2) \quad (24)$$

where R is the radius of the micelle [and again the parameters are dimensionless].

To find the extension from the surface for small curvatures, Milner and Witten[60] expand around h/R. In

the case of a micelle, however, the curvature is enormous and $h/R > 1$. As such, we must solve the equation numerically. [This analysis is valid near the surface of the micelle only if the PEG–lipid concentration in the micelle is not very high. The analysis is based on the assumption that the polymer solution near the surface is still semidilute. The assumption will not be valid for a 100% PEG–lipid because near the surface the monomer concentration will be very high and the chains will be strongly stretched. Here we are mainly interested in describing the micelle around the phase transition, and as we will show later, it occurs at not very high M % PEG–lipid. Thus we do not expect this assumption to invalidate the analysis presented here.]

After we calculate numerically the equilibrium extension, we find the energy of the "curved" brush, using the approach of Milner and Witten,[60] discussed in section 1.2. The free energy per unit area can be written as

$$F = \int_0^{\sigma} NA(\sigma')\, d\sigma' \tag{25}$$

We use this equation to obtain numerically the free energy per one polymer:

$$F_{curv} = F/\sigma \tag{26}$$

Each molecule, packed in the micelle is assigned a certain energy due to unfavorable packing G_{pack}. Szleifer *et al.*[34,35] study the molecular and thermodynamic properties of chains, packed in bilayers and micelles. They find, that the differences between the minimum chain free energies in different aggregates is small: the energy difference bilayers and spherical micelles G_{pack} is about $0.5kT$.[35]

By analogy, we can calculate the polymer free energy in the case of cylindrical micelles. In this case eq 23 will be written as

$$2\pi \int_R^{R+h} c(z) z\, dz = 2\pi RN\sigma \tag{27}$$

We find that if the deformation is cylindrical, the stress relaxation in the polymer system is smaller than in the case of spherical deformation. But the energy of unfavorable packing of the hydrocarbon tails should go down as well. G_{pack} for cylindrical micelles is of the order of $0.25kT$.[35]

To summarize, the free energy of the micelle per one polymer chain is

$$F_3 = F_{curv} + G_{pack}/M \tag{28}$$

Lastly, let us discuss the relation between the distance between points of grafting in the micelle D and the area per lipid molecule in the unperturbed bilayer A. Obviously

$$D^2 = A_2/M \tag{29}$$

where A_2 is the area in the micelle. Below we make a crude evaluation of the relation between A_2 and A.

We assume that the micelle can be divided in three regions (Figure 5): (1) a central core, (2) outer hydrocarbon chains, and (3) hydrated headgroups. The hydrocarbon core is built of melted hydrocarbon chains. In the outer region the hydrocarbon chains are not much changed as compared to their bilayer state. The lipid heads, however, are more expanded and hydrated. Thus we can assume that the neutral surface of the monolayer (the surface which does not change its area upon bending) lies just below the lipid heads. Then (in a spherical micelle)

$$\frac{A_2^{1/2}}{A^{1/2}} = \frac{\text{length of lipid molecule}}{\text{length of hydrocarbon tail}} \approx \frac{25\ \text{Å}}{20\ \text{Å}} \tag{30}$$

From this, for spherical micelles we find

$$A_2 = 1.56A \tag{31}$$

For cylindrical deformations the dimensions parallel to the axis do not change and so

$$A_2 = \frac{25}{20}A = 1.25A \tag{32}$$

This calculation is not precise because it neglects the additional area expansion due to the grafted polymer. The area change due to expansion, however, is not more than 5%[51] and is much smaller than the one due to the curvature, and we argue that this naive calculation gives a reasonable estimate of the lipid area in the micelle.

The energy F_3 is plotted for both cylindrical and spherical micelles for $A = 50$ Å^2 in Figure 7c,d for molecular weight 2000 and in Figure 8c,d for molecular weight 5000. For molecular weight 2000 at 14 M % the cylindrical micelle becomes the one with lowest energy as compared to the bilayer, interdigitated bilayer, and spherical micelle. The same occurs at 11 M % for 5000. The results from these calculations suggest that at these concentrations we will see a transition from bilayers to cylindrical micelles. If we continue increasing M above these values, we expect to see a transition from cylindrical to spherical micelles. Such transitions are predicted for molecular weight 2000 at 32 M % and for molecular weight 5000 at 18 M %.

In summary, these calculations show that the increase of the M % polymer–lipid will lead to a transition from bilayers to a cylindrical micellar phase at a certain concentration n_{tr}, which we call the thermodynamics crossover, and then from cylindrical to spherical micelles. An increase in N enhances the lateral repulsion in the polymer layer and thus leads to a monotonic decrease in n_{tr}. For low polymer molecular weights increasing the polymer–lipid concentration may result in the formation of interdigitated bilayers. Interdigitated bilayers, however, will not likely form for molecular weights 2000 and 5000. That is why we are particularly interested in the transition from bilayers to cylindrical micelles and we will study the mechanism of this transition. But first, let us talk about lipid bilayers.

3.2. Liquid Bilayers. For our consideration of liquid crystalline bilayers, we will assume that the polymer–lipid molecules can freely diffuse in the plane of the bilayer, as discussed above.

For high surface coverage the brush system for liquid crystalline bilayers is identical to the gel-phase one (the brushes can freely diffuse, but they are indistinguishable). As a result, the thermodynamics are similar to these of gel-phase lipids, but with two notable exceptions.

1. For liquid crystalline bilayers interdigitation of the hydrocarbon chains in the bilayers is not expected to occur, as the interdigitated phase has never been observed in liquid bilayers. This is because the area

per molecule A can take continuous values in order to minimize the energy (see section 3.1).

2. The parameters relevant to the liquid crystalline system are: $K_A = 200$ dyn/cm and $A = 65$ Å^2.[51] Our results (not presented here) show that the values of K_A and A have only a slight effect on the phase behavior determined by the polymorphic properties of the lipid molecules and on the thermodynamics crossover n_{tr}. (Note that the values of K_A and A determine the saturation limit n_{sat} (see eq 14).)

For low surface coverage the freely moving mushrooms can "collide" into each other. These collisions are a form of lateral interaction between the mushrooms and cost energy. This is a new effect, characteristic only of the liquid bilayer. To estimate its importance and possible consequences, we have to work out in detail the thermodynamics of this regime.

The simplest approach to modeling the case of low polymer surface coverage is as a van der Waals gas confined to a two-dimensional surface. This gas consists of polymer mushrooms, moving in the plane of the bilayer. [When hydrated, bilayer-forming lipids self-assemble into closed bilayer structures (vesicles), which define a closed 2D surface to which the mushrooms are confined.] When in contact, the polymer coils will not interpenetrate each other; they will act like hard spheres. The potential of interactions is assumed to be

$$U = \infty \quad \text{for} \quad z < R_F \tag{33}$$

where R_F is the Flory radius, a measure of the size of a polymer coil in solution and

$$U = 0 \quad \text{for} \quad z > R_F \tag{34}$$

This is justified by the fact that the energy density causing coil deformations is much higher than the pressure of this gas. For instance, for the dilute solution, the pressure is given by

$$\Pi_{dilute} = \frac{kT}{R^2} \tag{35}$$

where R is the average distance between coils. $R \gg R_F$.

In contrast, the pressure needed to deform a coil is of the order of [61]

$$\Pi = \frac{kT}{\xi^2} \tag{36}$$

where ξ is a characteristic length and $\xi < R_F$. Because $R \gg \xi$, it follows that $\Pi_{dilute} \ll \Pi$.

For the $2D$ mushroom gas the van der Waals equation of state is

$$\Pi(S - XR_F^2) = kTX \tag{37}$$

where Π is the lateral pressure, S is the area of one closed vesicle, and X is the number of mushrooms, confined to one side of the vesicle. R_F^2 is the area per mushroom. $(S - XR_F^2)$ then is the unoccupied, accessible area. Obviously, $X = S/D^2$, where D is the distance between the grafting points. Then

$$\Pi = \frac{kT}{D^2}\frac{1}{(1 - R_F^2/D^2)} = \frac{kT}{D^2}\left(1 + \frac{R_F^2}{D^2}\right) \tag{38}$$

for $R_F^2 \ll D^2$.

Second, let us calculate the chemical potential μ of one mushroom of this gas. The free energy is given by[62]

$$F = -XkT\left[\ln\left(n_q\frac{(S - XR_F^2)}{X}\right) + 1\right] \tag{39}$$

where n_q is the quantum concentration. It can be easily shown to be much larger than the actual mushroom concentration.

$$\mu = \frac{\partial F}{\phi X} = kT\left(\frac{S}{S - XF_F^2} - \ln\left(n_q\frac{(S - XR_F^2)}{X}\right) - 1\right) \tag{40}$$

$$= kT\left(\frac{R_F^2}{D^2} - \ln(n_q D^2(1 - R_F^2/D^2))\right)$$

for $R_F^2 \ll D^2$.

Let us consider the transition from bilayers to micelles. The chemical potential μ depends on the distance between the points of grafting. In the micelle according to (30) this distance is greater than in the bilayer. It is easy to show that $\mu_{micelle} - \mu_{bilayer} \propto 2kT\Delta D/D$, where ΔD is the increase in the distance between grafting points due to the curvature of the monolayer into a micelle (see the discussion about micelles). From (30) $\Delta D/D \propto 0.25$ and so $\mu_{micelle} - \mu_{bilayer} \propto 0.5kT$. These energies are small compared to the energies of micellization G_{pack}/M, since M is small. For instance for 1 M % $G_{pack}/M = 25kT$. The lateral pressure of the van der Waals mushroom gas is not likely to induce a phase transition to micelles.

4. Phase Transition from the Bilayer to the Micellar Phase

To extend our previous modeling, we will now allow for an arbitrary distribution of the two types of molecules (lipids and polymer–lipids) between the two phases—bilayer and micellar. Let us consider a sample: lipid/polymer–lipid mixture, hydrated in aqueous medium. Suppose we have Q amphiphilic molecules. Let P of them be polymer–lipid molecules. Obviously, P/Q is the molar polymer–lipid concentration in the sample. To describe the system, we will use two parameters: (1) P_1/P, the fraction of polymer–lipids in the bilayer phase, and (2) Q_1/Q, the fraction of total number of amphiphilic molecules in the bilayer phase. Obviously, $P_1/P = Q_1/Q = 1$ corresponds to the case when only the bilayer phase is present and $P_1/P = Q_1/Q = 0$ to the case when all the lipids are in a micellar phase. We assume that neither polymer–lipids or lipids exist as monomers; they are always grouped in aggregates (bilayers or micelles). [The analysis does not exclude the possibility for some lipids to exist as monomers. But if we know the critical micellar concentrations of the lipid and polymer–lipid and the water volume, we can calculate how much material is not incorporated in aggregates. So we can easily find the real molar fraction P/Q of the polymer–lipid in the lipid mixture.] Also, since the phase transition is supposed to occur as a result of the lateral interactions of the chains in the brush regime, we will consider only brush-covered micelles and bilayers.

The calculation of the free energy of the bilayer is done in analogy to the calculation in section 2. The minimum free energy of the polymer-grafted membrane

per one chain defined in the previous section is

$$F_1 = \frac{9kT\left(\frac{\pi^2}{12}\right)^{1/3} N\frac{a^{4/3}}{D^{4/3}}}{10}\left(1 - \frac{\frac{2}{5}kT\left(\frac{\pi^2}{12}\right)^{1/3} N\left(\frac{a^2}{D_1^2}\right)^{2/3}}{K_A D_1^2 + 2kT\left(\frac{\pi^2}{12}\right)^{1/3} N\left(\frac{a^2}{D_1^2}\right)^{2/3}}\right) \quad (41)$$

On the other hand the energy of a polymer chain grafted on a micelle F_{curv} is calculated numerically as a function of the degree of polymerization N and the distance between grafting points in the micelle D (see section 3.1). We will consider cylindrical micelles only because we identified that increasing the fraction of polymer–lipids in the lipid mixture is likely to induce a phase transition from bilayers to cylindrical micelles.

The free energy that we will study is the free energy of the system per one polymer–lipid molecule as a function of P_1/P and Q_1/Q (the two free parameters, which describe the material distribution between the two phases):

$$\frac{F}{P} = F_1\frac{P_1}{P} + F_{curv}\frac{(P - P_1)}{P} + \frac{G_{pack}(Q - Q_1)}{P} \quad (42)$$

The distances between grafting points D_1 in the unstretched bilayer and D in the micelle is related to the respective concentration through (13):

$$\frac{1}{D_1^2} = n_b\frac{1}{A} \quad (43)$$

and

$$\frac{1}{D^2} = n_m\frac{1}{A_2} \quad (44)$$

where n_b is the concentration in the bilayer and n_m is that in the micellar phase. A and A_2 are the area per lipid molecule in the unstretched bilayer and in the micelle, respectively.

The concentrations n_b and n_m are expressed through the parameters P_1/P, Q_1/Q, and P/Q as follows:

$$n_b = \frac{P_1}{Q_1} = \frac{P_1}{P}\frac{P}{Q}\frac{Q}{Q_1} \quad (45)$$

$$n_m = \frac{P - P_1}{Q - Q_1} = \frac{P}{Q}\frac{(1 - P_1/P)}{(1 - Q_1/Q)} \quad (46)$$

Using these equations, we find numerically the energy minimum of F/P with respect to P_1/P and Q_1/Q under the constraint that the concentration in the bilayer phase n_b does not exceed the limit due to the critical material parameters of the bilayer (saturation limit n_{sat} (14)).

Here we will present the results for molecular weight 2000 ($N = 46$). For the area per lipid molecule in the unstretched bilayer we use $A = 50$ Å^2, $K_A = 1000$ dyn/cm and $A = 65$ Å^2, $K_A = 200$ dyn/cm for the gel-phase and liquid system, respectively. In Figures 10 and 11 for the gel-phase and liquid bilayer, respectively, we plot the following.

1. Location of the energy minimum (P_1/P and Q_1/Q) of the system as a function of the polymer–lipid concentration in the sample. ($P_1/P = Q_1/Q = 1$ corresponds to the bilayer phase, $P_1/P = Q_1/Q = 0$ to the micellar phase.) The solid line shows the value of P_1/P and the dashed line the value of Q_1/Q for which the energy minimum is achieved.

2. Polymer–lipid concentration in the bilayer versus polymer–lipid concentration in the sample.

3. Polymer–lipid concentration in the micellar phase versus polymer–lipid concentration in the sample.

The location of the energy minimum shows which phase is most probable to occur. Our calculations show that the energy difference between the two phases is of the order of several kT. Because this is a relatively small difference, the higher energy phase, although not predominant, still might exist due to the thermal

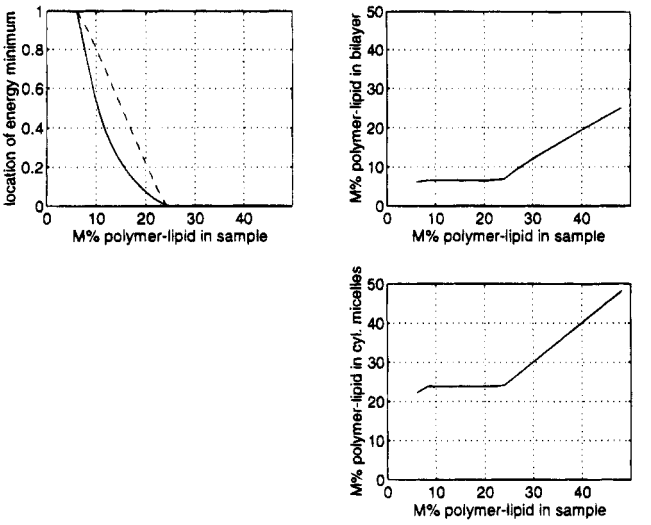

Figure 10. Effect of lipid polymorphism on bilayer to micelle phase transition for gel-phase bilayers ($A = 50$ Å^2, $K_A = 1000$ dyn/cm, $G_{pack}^{cyl} = 0.25kT$, $a = 3.5$ Å). (a) Location of energy minimum for a mixed bilayer/micelle system. 1 corresponds to bilayers; 0, to micelles (see text). (b) Polymer–lipid concentration in the bilayer as a function of polymer–lipid concentration in the sample. (c) Polymer–lipid concentration in the micelles as a function of polymer–lipid concentration in the sample.

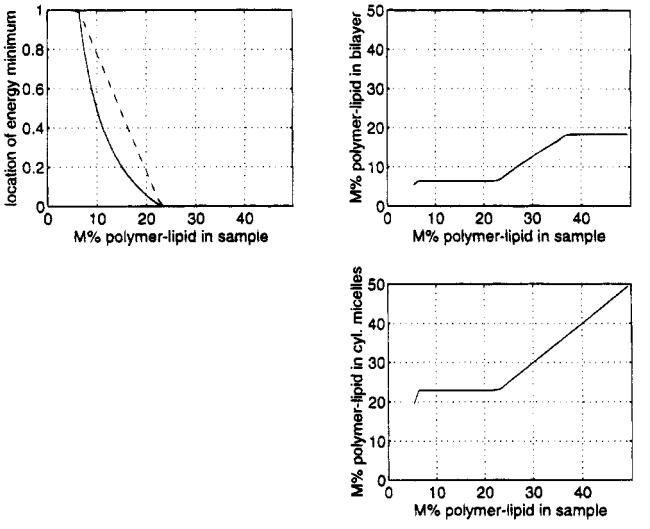

Figure 11. Effect of lipid polymorphism on bilayer to micelle phase transition for liquid bilayers ($A = 65$ Å^2, $K_A = 200$ dyn/cm, $G_{pack}^{cyl} = 0.25kT$, $a = 3.5$ Å). (a) Location of energy minimum for a mixed bilayer/micelle system. 1 corresponds to bilayers; 0, to micelles (see text). (b) Polymer–lipid concentration in the bilayer as a function of polymer–lipid concentration in the sample. (c) Polymer–lipid concentration in the micelles as a function of polymer–lipid concentration in the sample.

fluctuations of the system. That is why we plot the polymer–lipid concentrations in the bilayer and in micelles for the whole range of polymer–lipid concentrations in the sample that we are studying.

4.1. Gel-Phase Bilayers. For gel-phase bilayers we use values of $A = 50$ Å^2 and $K_A = 1000$ dyn/cm. The results are shown in Figure 10.

From Figure 10a we see that upon an increase in the concentration of polymer–lipid in the sample the energy minimum of the system gradually moves from a bilayer into a micellar phase.

For low concentrations the dominant phase is the bilayer. For high concentrations the micellar phase is expected to dominate. In the transition region the energy mimimum occurs when the system is a mixture of bilayers and micelles. Increasing the concentration has the effect of decreasing the probability of the formation of bilayers.

In the bilayer and the micellar phase the polymer–lipid concentrations equal the one in the sample. In the transition region there is a mixed phase where bilayers and micelles have the same energy and therefore coexist. The two populations, however, do not have the same concentrations of polymer lipids; in the bilayer, the concentrations are smaller than the one in the sample and in the micelles they are larger than the one in the sample.

We see that at low concentrations the polymer–lipid concentration in the bilayer phase increases linearly with the increase of the polymer–lipid concentration in the sample. In the transition region the polymer–lipid concentration in the bilayer levels off at about $n_{tr} = 7$ M %. Increasing the concentration in the sample does not change the concentration in the bilayer. The effect is the progressive solubilization of the bilayers and the appearence of micelles which bear a higher polymer–lipid concentration. The maximal concentration of polymer–lipids in the bilayer n_{sat} given by (14) is not shown on the plot. It is about 37 M %.

4.2. Liquid Bilayers. For liquid bilayers we assume values of $A = 65$ Å^2 and $K_A = 200$ dyn/cm. The results are shown in Figure 11.

The difference for liquid compared to gel bilayers is that for polymer–lipid concentrations in the sample less than 50% we see two plateaus in the polymer–lipid concentration in the bilayer. Since K_A is about 5 times smaller for liquid bilayers than for gel-phase bilayers, the maximal concentration due to the critical material properties n_{sat} is much lower (about 18 M %). This corresponds to the higher plateau. The lower plateau in the polymer–lipid concentration in the bilayer occurs at about $n_{tr} = 7$ M %. It indicates a transition from polymer-poor bilayers to polymer-rich micelles as for gel-phase bilayers.

Thus we see that both gel-phase and liquid bilayers undergo a gradual transition to cylindrical micelles. The difference in the numerical value of n_{sat} below and above the liquid to gel phase transition is due to the different molecular packing of the lipid molecules in the bilayer. This different molecular packing determines the different values of K_A and A of liquid crystalline and gel-phase bilayers and thus the different n_{sat}. The values of K_A and A, however, have no major effect on n_{tr}. We obtained this result for both molecular weights-2000 and 5000 (results for 5000 not shown). Increasing N leads to a monotonic decrease in both n_{sat} and n_{tr}. A similar result is obtained when the transition from bilayers to spherical micelles is considered (results not shown). The existence of a broad two-phase region for which micelles and bilayers coexist has been proven experimentally (A. Kenworthy, S. Simon, and T. J. McIntosh, *Biophysical Journal*, submitted).

5. Discussion

This work shows that increasing the molar concentrations of polymer-grafted lipids in phospholipid bilayers leads to a phase transition from a bilayer to a micellar phase. We do the calculations for polymer molecular weights 2000 and 5000—products used in the preparation of drug-carrying liposomes for therapeutical purposes.

Our work can be summerized as follows.

(1) We find the absolute maximum polymer–lipid concentration that can be achieved in the bilayer. It is determined by the critical material properties of the bilayer.

(2) We derive the free energy density of different polymer–lipid/lipid/water phases and identify the bilayer to micelle transition as the most probable transition to occur upon an increase in the amount of polymer–lipid.

(3) We write the free energy of the polymer–lipid/lipid/water system (bilayers + micelles) as a function of the polymer–lipid concentration.

(4) We search for the minimum of this free energy under the constraint obtained in (1).

For DSPC and SOPC bilayers we find that, upon an increase in the concentration of polymer–lipid in the sample the energy minimum gradually moves from bilayer into a micellar phase. The proposed theoretical model allows us to predict both the polymer–lipid concentration in the bilayer and the polymer–lipid concentration in the micellar phase as a function of the polymer–lipid concentration in the sample. The distribution of material between the two phases depends on the elastic constants of the bilayer, the molecular weight of the polymer and the molecular characteristics of the lipids.

For DSPC and SOPC bilayers we obtained $n_{tr} < n_{sat}$. If the lipid bilayer is extremely soft and deformable, however (for instance, if there are multiple double bonds in the hydrocarbon chains as in the case of DAPC), K_A will be very small and we can expect the saturation due to the material properties to occur before the bilayer to micelle transition. The experiment verification of the proposed phase behavior will be published elsewhere (K. Hristova, A. Kenworthy, D. Needham, T. J. McIntosh, in preparation).

The work shows that the polymer–lipid/lipid system has a complex phase diagram. Depending on the parameters of the system—G, G_{pack}, N, M—we can have bilayers, interdigitated bilayers, or micelles of different shapes. The energy density difference between the phases is of the order of several kT and depending on the system parameters it can change sign or become zero: different phases can coexist.

The major result of this work is that the polymer–lipid concentration in the bilayer phase does not necessarily equal the one in the sample. It is true only for polymer–lipid concentrations less than n_{tr} and n_{sat}. Increasing the PEG–lipid concentration above this limit will actually deteriorate the in-vitro performance of the drug-carrying liposomes. This is of extreme importance in liposome preparation for therapeutic applications and it has been observed in in-vivo studies.[8]

We note that in this analysis we are considering only planar bilayers and micelles. In reality small vesicles with monolayers of different composition may also form.[46] Experimentally, we observe that the result of hydration of a mixture of PEG–lipids and lipids (for relatively low PEG–lipid concentrations, i.e. in the bilayer phase) is the formation of giant multilamellar vesicles. The fraction of the small vesicles (the innermost bilayer leaflets) in the bilayer phase is small. So we think that the proposed modeling gives a good understanding of the solubilization of the bilayer phase.

At the end we emphasize again that the effects of incorporated polymer–lipid on the lipid structure resembles the effect of incorporated lysolipids or other conical amphiphilic molecules.[46] For instance, it has been shown that the incorporation of conical lysolecithin molecules into lecithin bilayers destabilizes the bilayer and leads to micelle formation.[63] In the polymer–lipid system, however, because of the large size and the hydrophilic nature of the grafted polymer the properties of the polymer must be explicitly taken into account. Thus instead of treating the polymer–lipid molecule as one huge conical molecule we treat the lipid/polymer–lipid membranes as built up of two distinct components: the bilayer, deformed due to the presence of the polymer, and the polymer layer grafted on the bilayer surface. In this model, it is the mutual dependence of the two components of the composite membrane which leads to and determines the characteristics of the lamellar to micellar phase transition.

Acknowledgment. K.H. would like to thank Thomas J. McIntosh, Anne Kenworthy, Jacob N. Israelachvili, and Joshua Socolar for the helpful and enjoyable discussions.

References and Notes

(1) Blume, G.; Cevc, G. *Biochim. Biophys. Acta* **1990**, *1029*, 91.
(2) Klibanov, A.; Maruyama, K.; Torchilin, V.; Huang, L. *FEBS Lett.* **1990**, *268*, 235.
(3) Mori, A.; Klibanov, A.; Torchilin, V.; Huang, L. *FEBS Lett.* **1991**, *284*, 263.
(4) Needham, D.; Hristova, K.; McIntosh, T.; Dewhirst, M.; Wu, N.; Lasic, D. *J. Liposome Res.* **1992**, *2*, 411.
(5) Papahadjopoulos, D.; Allen, T.; Gabizon, A.; Mayhew, E.; Matthay, K.; Huang, S.; Lee, K.; Woodle, M.; Lasic, D.; Redemann, C.; Martin, F. *Proc. Natl. Acad. Sci. U.S.A.* **1991**, *88*, 11460.
(6) Senior, J.; Delgado, C.; Fisher, D.; Tilcock, C.; Gregoriadis, G. *Biochim. Biophys. Acta* **1991**, *1062*, 77.
(7) Mayhew, E.; Lasic, D.; Babbar, S.; Martin, F. *Int. J. Cancer* **1992**, *51*, 302.
(8) Woodle, M.; Lasic, D. *Biochim. Biophys. Acta* **1992**, *1113*. 171.
(9) Williams, S.; Alosco, T.; Mayhew, E.; Lasic, D.; F. J. M.; Blankert, R. *Cancer Res.* **1993**, *53*, 3964.
(10) Litzinger, D.; Huang, L. *Biochim. Biophys. Acta* **1992**, *1127*, 249.
(11) Torchilin, V.; Klibanov, A.; Huang, L.; O'Donell, S.; Nossiff, N.; Khaw, B. *FASEB J.* **1992**, *6*, 2716.
(12) Needham, D.; McIntosh, T.; Lasic, D. *Biochim. Biophys. Acta* **1992**, *1108*, 40.
(13) Kenworthy, A.; McIntosh, T.; Needham, D.; Hristova, K. *Biophys. J.* **1993**, *64*, A348.
(14) Hristova, K.; Needham, D. *J. Colloid Interface Sci.* **1994**, *168*, 302.
(15) Hristova, K.; Needham, D. *Liq. Cryst.*, in press.
(16) Alexander, S. *J. Phys. (Paris)* **1977**, *38*, 983.
(17) de Gennes, P. *Macromolecules* **1980**, *13*, 1069.
(18) Milner, S.; Witten, T.; Cates, M. *Europhys. Lett.* **1988**, *5*, 413.
(19) Milner, S. *Europhys. Lett.* **1988**, *7*, 695.
(20) Milner, S.; Witten, T.; Cates, M. *Macromolecules* **1988**, *21*, 2610.
(21) Ajdari, A.; Liebler, L. *Macromolecules* **1991**, *24*, 6805.
(22) Dan, N.; Wang, Z.-G.; Safran, S. *J. Chem. Phys.* **1991**, *94*, 679.
(23) Dan, N.; Tirrel, M. *Macromolecules* **1993** *26*, 637.
(24) Barnevald, P.; Scheutjens, J.; Lyklema, J. *Langmuir* **1992**, *8*, 3122.
(25) Szleifer, I.; Kramer, D.; Ben-Shaul, A.; Gelbart, W.; Safran, S. *J. Chem. Phys.* **1990**, *92*, 6800.
(26) Petrov, A.; Bivas, I. *Prog. Surf. Sci.* **1984**, *16*, 389.
(27) Bivas, I.; Hanusse, P.; Bothorel, P.; Lalanne, J.; Aguerre-Chariol, O. *J. Phys. (Paris)* **1987**, *48*, 855.
(28) Faucon, J.; Mitov, M.; Meleard, P.; Bivas, I.; Bothorel, P. *J. Phys. (Paris)* **1989**, *50*, 2389.
(29) Cantor, R.; McIlroy, P. *J. Chem. Phys.* **1989**, *90*, 4423.
(30) Cantor, R.; McIlroy, P. *J. Chem. Phys.* **1989**, *90*, 4431.
(31) Cantor, R.; McIlroy, P. *J. Chem. Phys.* **1989**, *91*, 416.
(32) Cantor, R. *J. Chem. Phys.* **1993**, *99*, 7124.
(33) Ben-Shaul, A.; Szleifer, I.; Gelbart, W. *Proc. Natl. Acad. Sci. U.S.A.* **1984**, *81*, 4601.
(34) Ben-Shaul, A.; Szleifer, I.; Gelbart, W. *J. Chem. Phys.* **1985**, *83*, 3592.
(35) Ben-Shaul, A.; Szleifer, I.; Gelbart, W. *J. Chem. Phys.* **1985**, *83*, 3612.
(36) Szleifer, I.; Ben-Shaul, A.; Gelbart, W. *J. Chem. Phys.* **1986**, *85*, 5345.
(37) Szleifer, I.; Ben-Shaul, A.; Gelbart, W. *J. Chem. Phys.* **1987**, *86*, 7094.
(38) Semenov, A. *Sov. Phys. JETP* **1985**, *61*, 733.
(39) Liebler, L. *Macromolecules* **1980**, 13, 1602.
(40) Helfand, E.; Wasserman, Z. *Macromolecules* **1976**, *9*, 879.
(41) Shim, D.; Marques, C.; Cates, M. *Macromolecules* **1991**, *24*, 5309.
(42) Wang, Z.-G.; Safran, S. *J. Phys. (Paris)* **1990**, *51*, 185.
(43) Dan, N.; Safran, S. *Europhys. Lett.* **1993**, *21*, 975.
(44) Israelachvili, J. *Intermolecular and Surface Forces*; Academic Press: San Diego, CA, 1985.
(45) Lin, T.-L. *J. Colloid Interface Sci.* **1992**, *154*. 444.
(46) Pincus, S. P.; Andelman, D. *Science* **1990**, *248*, 354.
(47) Cevc, G.; Marsh, D. *Phospholipid bilayers*; John Wiley and Sons: New York, 1987.
(48) Marsh, D. *Handbook of Lipids Bilayers*; CRC Press, Inc.: Boca Raton, FL, 1990.
(49) Tanford, C. *The Hydrophobic Effect*; John Wiley: New York, 1980.
(50) Evans, E.; Skalak, R. *Mechanics and Thermodynamics of Biomembranes*; CRC Press, Inc.: Engelwood Cliffs, NJ, 1980.
(51) (a) Needham, D.; Nunn, R. *Biophys. J.* **1990**, *58*, 997. (b) In a different paper (A. Kenworthy, K. Hristova, D. Needham, and T. J. McIntosh (*Biochemistry*, submitted)) we measure the repulsive forces between PEG-grafted bilayers and model these forces by extending current polymer theories. Comparing theoretical predictions and data, we find that the optimal value for a is about 3.5 Å, which happens to be the size of the chemical mer CH_2-CH_2-O. This is not surprising, since the C–O is very flexible, as compared to the rigid C–C bond.
(52) Evans, E.; Needham, D. In *Physics of Amphiphilic Layers*; Meunier, J., Langevin, D., Boccara, N., Eds.; Springer Proceedings in Physics; Springer Verlag: Berlin, 1988.
(53) Evans, E.; Needham, D. *Macromolecules* **1988**, *21*, 1822.
(54) Milner, S.; Witten, T.; Cates, M. *Macromolecules* **1989**, *22*, 853.
(55) Flory, P. *Principles in Polymer Chemistry*; Cornell University Press: Ithaca, NY, 1969.
(56) Ranck, J.; Keira, T.; Luzzati, V. *Biochim. Biophys. Acta* **1977**, *488*, 432.
(57) McDaniel, R.; McIntosh, T.; Simon, S. *Biochim. Biophys. Acta* **1983**, *731*, 97.
(58) Simon, S.; McIntosh, T. *Biochim. Biophys. Acta* **1984**, *773*, 169.
(59) Shaw, D. *Introduction to Colloid and Surface Chemistry*; Butterworth-Heinemann Ltd.: Oxford, U.K., 1966.
(60) Milner, S.; Witten, T. *J. Phys. (Paris)* **1988**, *49*, 1951.
(61) de Gennes, P. *Scaling Concepts in Polymer Physics*; Cornell University Press: Ithaca, NY, 1985.
(62) Kittel, C.; Kroemer, H. *Thermal Physics*; W. H. Freeman and Co.: San Francisco, 1980.
(63) Mitov, M. IV Liquid Crystal Conference Soc. Countries, Tbilisi, 1981.

MA941169Y